A comparison of actuator disc and BEM models in CFD simulations for the prediction of offshore wake losses

Luca Lavaroni[1,3], Simon J Watson[2], Malcolm J Cook[1] and Mark R Dubal[3]

[1] School of Civil and Building Engineering Loughborough University, Leicestershire, LE11 3TU, UK
[2] CREST, School of Electronic, Electrical and Systems Engineering, Loughborough University, Leicestershire, LE11 3TU, UK
[3] E.ON New Build & Technology Limited, Technology Centre, Ratcliffe-on-Soar, Nottinghamshire, NG11 0EE, UK

E-mail: L.Lavaroni@lboro.ac.uk

Abstract.
In this paper computational fluid dynamics (CFD) simulations are performed using ANSYS CFX to compare wake interaction results obtained from two rotor modelling methodologies: the standard actuator disc and the blade element momentum model (BEM). The unsteady simulations embed Coriolis forces and neutral stability conditions in the surface layer and stable conditions in the free stream. The BEM method is implemented in the CFD code through a pre-processing set of files that employs look-up tables. The control system for the wind turbines is considered through look-up tables that are constructed based on operational wind farm data. Simulations using the actuator disc and BEM methodologies have been performed using a number of different turbulence models in order to compare the wind turbine wake structure results. The use of URANS and LES numerical methods, coupled with the two different methodologies of representing the turbine, enables an assessment to be made of the details required for varying degrees of accuracy in computing the wake structures. The findings stress the importance of including the rotation of the wake and the non-uniform load on the rotor in LES simulations to account for more accurate turbulence intensity levels in the near wake.

1. Introduction

The study of wakes in wind farms has been a popular topic of research during the last two decades, gaining momentum from computational fluid dynamics (CFD) methods that allow more complex modelling of the physics of the wake flow than the empirical models. In particular, advanced turbine rotor modelling techniques and turbulence methods have been developed to obtain increased accuracy of the flow in wind farms.

Researchers have looked at the flow through wind farms in the atmospheric boundary layer with different methods. Past studies have employed Reynolds-Averaged Navier-Stokes (RANS) [1] [2] showing that the method is unable to model the turbulent propagation of the eddies accurately. Large eddy simulation (LES) is better suited to study the turbulence structures as

it resolves the large scales of the flow field solutions while it models the smallest scales through the use of a sub-grid scale (SGS) model.

As for the rotor modelling techniques, Jimenez et al [3] [4] have suggested a simplified LES Smagorinsky model using an actuator disc with no detail on the blades. Good agreement of this study with experimental results has been obtained with regard to the turbulence characteristics. In a study by Calaf et al [5] LES simulations with a Lagrangian scale-dependent dynamic model have also been performed by employing a simplified disc method. Sørensen et al [7] [6] [8] have used the actuator disc technique solving the unsteady Euler equations with constant and also non-uniform load on the rotor. In order to spread the load over the rotor more evenly, a regularisation kernel has been implemented: the type of kernel used indicates a compromise between the stability and the accuracy of the simulation. A study of the Blade Element Momentum (BEM) method has been undertaken by Madsen et al [9] [10], suggesting a correction at the tip of the rotor. Simulations employing the actuator disc with and without rotation of the flow have been performed in LES by Porté-Agel et al [11] [19]: the findings have highlighted the importance of the rotation of the disc in order to capture the turbulence intensity levels at the top tip of the rotor, while the actuator disc under-estimates the wake losses in the near wake. The two rotor modelling techniques tend to give similar results further downstream.

The objective of the present study was to compare URANS and LES simulation results employing the standard actuator disc and the actuator disc with BEM models, in neutral atmospheric stability conditions and including the effect of the Coriolis force. The BEM model makes use of the wind turbine control system through wind farm operational data. Data obtained from wind tunnel measurements has been used to validate the results from the CFD models. The goal of the paper is to validate a generic behaviour of the wake. Hence the wind tunnel measurements that represent a large offshore turbine were chosen to be compared with the CFD models, although the airfoil data are different and therefore a detailed comparison of the turbine aerodynamics is not possible.

2. Methodology

2.1. Wind tunnel measurements

The wind tunnel measurements made by Hancock et al [12] in neutral atmospheric stability conditions have been used to validate the CFD models. In particular, profiles of wind speed and turbulence intensity at 1, 3 and 5 rotor diameters (D) downstream of the rotor in full wake conditions have been used to compare with the results obtained from the computations in this work. The model turbine employed for the wind tunnel measurements has been scaled down by a factor of 300. This corresponds to a hub height and rotor diameter of 90 and 120 m respectively. The wind tunnel roughness values were consistent with modelling offshore conditions. It was found that the thrust coefficient obtained through the blade element ignoring tip loss was $\sim$0.53. However, it was possible to quantify the effect of the tip loss with the wake measurements in a uniform flow, obtaining CT$\sim$0.48. The CFD models used a free stream wind speed of 12.5 m/s that corresponds to a CT$\sim$0.5 on the thrust coefficient curve for the Siemens Bonus 2.3MW wind turbine. Although the turbines are different, the main goal of the paper was to study the generic behaviour of the wake propagation downstream of a wind turbine in a qualitative way.

2.2. Numerical method

Numerical simulations are performed using the CFD commercial software ANSYS CFX [17]. A set of pre and post-processing tools called WindModeller is employed to automate the set-up of the boundary conditions and the overall numerical simulation. URANS and LES models are performed to capture the large spectrum of time scales that characterises the flow field.

2.2.1. URANS In this work, the URANS solutions are obtained through the standard two-equation $k-\omega$ Shear-Stress-Transport (SST) turbulence model developed by Menter [13]. The constants of the model are defined in Table 1.

Table 1. Coefficients used in the $k-\omega$ SST model [13]

C_μ	t_{dexp1}	t_{dexp2}	$C_{\epsilon 1}$	$C_{\epsilon 2}$	σ_{k1}	$\sigma_{\omega 2}$	σ_{k2}	$\sigma_{\omega 2}$	β_1	β_2
0.09	1.2	1.087	1.44	1.92	1.176	2.0	1.0	1.168	0.075	0.0828

2.2.2. Zonal LES Zonal LES is an infrastructure that allows the combination of two different treatments of turbulence in a pre-processing stage [14]. In this work, the Scale Adaptive Simulation (SAS)-SST model is used in the coarse mesh region of the computational domain, while Smagorinsky LES is activated in the most refined area in which the turbine rotors are located. The LES region is defined through an expression (step function) in the CFX code that switches on a forcing term in the momentum and turbulence equations. In addition, the interface activated between the two regions allows the transfer of the modelled turbulent kinetic energy into resolved turbulent kinetic energy. The synthetic velocity fluctuations injected at the interface, in a non-critical region of the flow, maintain their statistical properties (time and length scales) unchanged between the domain of the upstream SAS-SST model and the LES operated zone [15]. The harmonic flow generator is defined via a Fourier series of N modes to express the velocity fluctuations $\overrightarrow{u'}$:

$$\overrightarrow{u'} = 2\sum_{n=1}^{N} \widehat{u}_n cos(\overrightarrow{k}_n \cdot \overrightarrow{x} + \omega t + \psi_n)\sigma_n \tag{1}$$

where $\widehat{u}_n$ determines the amplitude of the mode, σ_n is the unity direction vector and ψ_n the random mode phases.

2.3. Rotor modelling techniques
In this work, the simplification of the wind power extraction with a turbine is made by means of two models that are compared to study the wake propagation downstream of the rotor: a) the standard actuator disc without rotation and b) the actuator disc with rotation implemented through the Blade Element Momentum (BEM) model that accounts for airfoil data. The modelled wind turbine is a combi stall regulated Siemens-Bonus 2.3 MW with a hub height of 68.8 m and a rotor diameter of 82.4 m, as installed at the Nysted wind farm site.

2.3.1. Standard actuator disc The actuator disc method makes use of equivalent forces in order to represent the turbine rotor, while a full set of Navier Stokes equation resolve the flow field in the surroundings. The main benefit of this simplified technique is that the the viscous airfoil boundary layer is not resolved, hence the resolution of the grid can be coarser compared to a full CFD simulation. With regard to the constantly loaded actuator disc, it represents the most common technique in which body forces are spread over a permeable disc that is characterised by zero thickness. It provides a momentum sink in a cylindrical volume that surrounds the turbine. It has been used in many studies in order to analyse and validate the momentum theory. The force $\mathbf{f}$ that is exerted by the rotor on the flow is expressed in terms of the thrust coefficient C_T and its equation for an actuator disc that is uniformly loaded is as follows:

$$\mathbf{f} = \frac{1}{2}\rho A_D V_{ref}^2 C_T \tag{2}$$

where ρ is the air density, A_D is the rotor area and V_{ref} is the free-stream wind speed at hub height upstream of the rotor. The turbine thrust curve, the turbine hub height and diameter are provided as the input for the computation.

2.3.2. Actuator disc with BEM model The BEM model defines the blades aerodynamically as two-dimensional airfoils. The local flow and the lift and drag characteristics of the airfoil are used to compute the forces acting on the blade. In particular, the resulting force f_{2D} per unit rotor area $dA = 2\pi r dr$ is as follows:

$$f_{2D} = \frac{d\mathbf{F}}{dA} = \frac{\rho V_{rel}^2}{2}\frac{Bc}{2\pi r}(C_L\mathbf{e_L} + C_D\mathbf{e_D}) \tag{3}$$

where B indicates the number of blades, c is the blade chord length, r is the radial length, V_{rel} is the local relative velocity, C_L and C_D are the lift and drag coefficients and $\mathbf{e_L}$, and $\mathbf{e_L}$ are the direction of the unit vector for the lift and drag forces. The local relative velocity V_{rel} is obtained from the components of absolute velocity in axial and tangential directions $V_{rel} = (V_x,\ r\Omega\text{-}V_\theta)$ where Ω is the angular velocity of the turbine. The turbine hub is defined as a blockage through its radius, below which no sources are calculated. The hub sink terms are then subtracted from the momentum sources computed from the sum of the lift and drag forces in X, Y and Z directions. Also, a correction for the source volume against the swept volume is applied. The tables for the drag and lift coefficients, the blade chord, the blade relative thickness and the hydrodynamic twist of the NACA 63.xxx and FFA.xxx are derived using the manufacturer's aerofoil data based on CFD and wind tunnel measurements. The control system for the wind turbines is considered through the turbine pitch angle and the shaft angular velocity. The look-up tables for these parameters are constructed based on operational Nysted offshore wind farm data recorded from 2006 to 2008. The curves of the pitch angle and the shaft angular velocity, that depend on the axial wind speed, are smoothed and the look-up tables are created on the basis of the best fit line.

2.4. Model set-up

The model implements neutral atmospheric stability conditions in the surface layer and stable conditions in the free stream at a boundary layer altitude of 500m. The turbulent transport and vertical momentum equations make use of the potential temperature to account for the buoyancy force [17]. The Coriolis force is also added to the model through the momentum equations, assuming that the geostrophic balance is satisfied by the free stream flow. Coriolis force is included in the model in order to produce a consistent boundary layer which is neutral in the boundary layer and stable in the free stream. The inflow velocity profiles make use of the similarity theory developed by Zilitinkevich et al. [16] Expressions for the turbulent kinetic energy, k, and the dissipation rate of turbulent kinetic energy, ϵ , are then used to achieve preservation of the profiles defined at the inlet over the development of the boundary layer [17]. In order to achieve sufficient temporal resolution, the maximum Courant Friedrichs Levy (CFL) number is limited to be smaller than 1 through an adaptive time step selection.

2.5. Computational domain

The cylindrical computational domain has a 3 km radius, 1 km height and comprises of two 2.3 MW Siemens Bonus wind turbines located at the distance of 6 rotor diameters (D), as in Fig 1. Although two turbines are present in the computational domain, only one turbine has been used in the wind tunnel, therefore all comparisons with that data are made with reference to the most

upstream rotor. The mesh consists of approximately 25 million cells and the most refined region (22 million cells) in the domain has an extension of 20 D and 5 D in the streamwise and spanwise directions respectively, and 5 D in height. The LES zone is generated using a 1m mesh spacing defined at the ground boundary, with geometrical progression to the top of the domain. The resulting aspect ratio of the cells at the rotor location is close to 1. The radius of the cylindrical domain is 3km and the height is 1km. Outside of the zonal LES region the mesh had a 20m resolution in the horizontal, while vertically the first six layers from the surface boundary had thicknesses of 2m, 2m, 3m, 3m, 5m and 5m, respectively, and a geometrical progression of 1.3 to distribute the grid lines in the vertical direction. With regard to the mesh for the zonal LES simulation, it is assumed that an acceptable resolution is achieved when the resolved turbulent kinetic energy is not less than 80% of the total turbulent kinetic energy. This criterion is satisfied through the ratio $L/\Delta>12$, where L is an integral turbulence length scale and Δ is the filter width (related to local grid size). The value of the ratio L/Δ is higher than 12 throughout the refined region, thus the mesh is considered sufficiently refined. In the zonal LES simulation, the modelled turbulent kinetic energy is transferred into resolved turbulent kinetic energy through an interface between the SAS-SST and the LES regions.

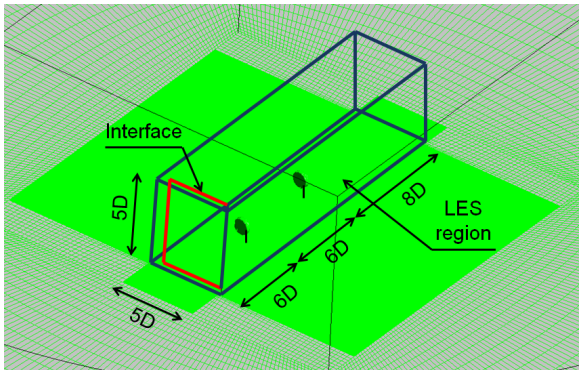

Figure 1. Computational domain close up, showing the interface between SAS-SST and LES regions.

2.6. Boundary conditions
The boundary conditions applied to the inlet are: turbulent kinetic energy k, turbulent dissipation ϵ, Dirichlet type on velocity and Neumann on pressure. A prescribed static pressure and Neumann conditions on velocities and turbulence quantities are applied to entrainment openings at the downstream boundaries of the domain and at the top of the domain.

3. Results and discussions
In the present work, numerical simulations are performed of the full scale turbine at high Reynolds number and are carried out with URANS and LES models using the actuator disc in the cases a) without rotation and constant thrust coefficient over the turbine rotor and b) with the BEM model accounting for rotation of the turbine and uneven thrust. The convergence of the residuals is statistically achieved, although longer run time would be beneficial in order to improve the convergence statistics. The simulation ran for 85 seconds simulation time, the time step was 0.02 seconds. The results obtained from the CFD simulations are then compared to wind-tunnel measurements. In particular, the propagation of the wakes is analysed through the time-averaged streamwise velocity and the time averaged turbulence intensity, extracted at 2D upstream of the rotor and 1D, 3D and 5D downstream of the rotor. Also, contours for the cross-section at 1D downstream of the rotor are provided to visualise the wake differences.The surface in the vertical profiles is located at Z/D=-0.63, while it is at Z/D=0 for the cross-sections.

In Figs. 2 and 3 the vertical profiles of normalised time-averaged velocity U/U_0 and turbulence intensity I are plotted for the four computational models and the wind tunnel measurements. The profiles show good agreement with the wind tunnel measurements with regard to the time-averaged velocity, apart from the ground region where all model shear values are higher than the wind tunnel data. Similarly, the turbulence intensity profiles in Fig. 3 present acceptable agreement above the ground region but lower turbulence intensity (∼5%) for the models than the wind tunnel data (∼7.5%) in the ground area.

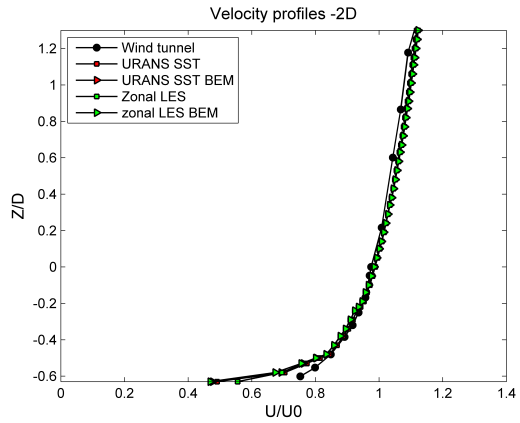

Figure 2. Normalised vertical profiles of time averaged-velocity U/U_0 at 2D upstream of the turbine.

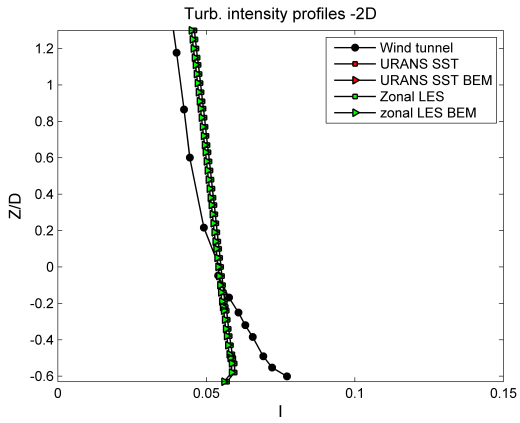

Figure 3. Normalised vertical profiles of time averaged-turbulence intensity at 2D upstream of the turbine.

The velocity profiles in Fig. 4 clearly show that the URANS and zonal LES models with actuator disc are not able to account for the rotor geometry, producing a linear velocity deficit over the whole turbine. This behaviour is explained by the lack of rotation caused by the turbine and the constantly distributed thrust over the rotor. On the contrary, the models incorporating the BEM model present higher velocity at the nacelle height (Z/D=0) and lower velocity at the tips of the rotor, in agreement with the wind tunnel measurements.

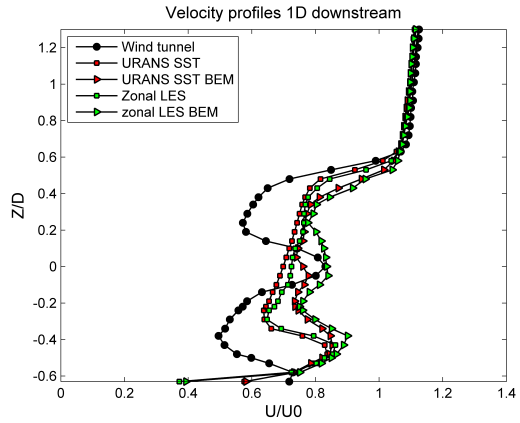

Figure 4. Normalised vertical profiles of time averaged-velocity U/U_0 at 1D downstream of the first turbine.

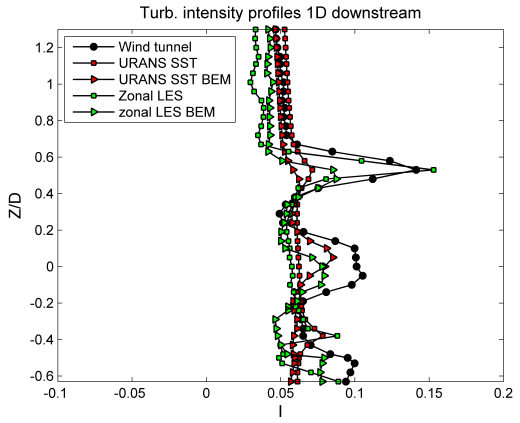

Figure 5. Normalised vertical profiles of time averaged-turbulence intensity at 1D downstream of the first turbine.

The velocity deficit is mainly under-predicted by all the models: in particular, the BEM

models give good agreement at the nacelle height but under-predict the velocity deficit at the tips.

Fig. 5 shows the profiles of turbulence intensity I at 1D downstream of the rotor: it can be noticed that the wind tunnel measurements present a peak of turbulence intensity at the top tip height. This is in agreement with previous findings by Chamorro et al. [18] and Wu et al. [19]. It can be seen that the increase of turbulence intensity at the top tip is captured by the zonal LES models, while the higher turbulence at the hub height is only observed for the models incorporating BEM, as expected because of the modelled nacelle blockage.

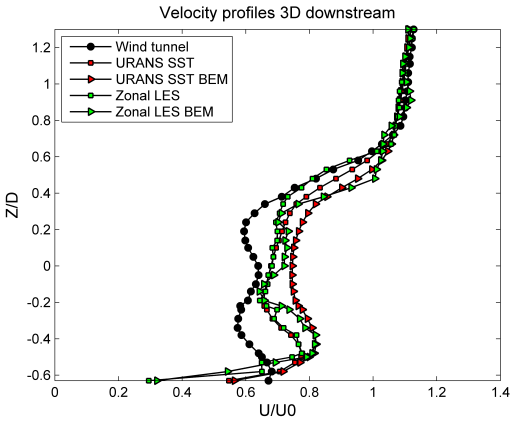

Figure 6. Normalised vertical profiles of time averaged-velocity U/U_0 at 3D downstream of the turbine.

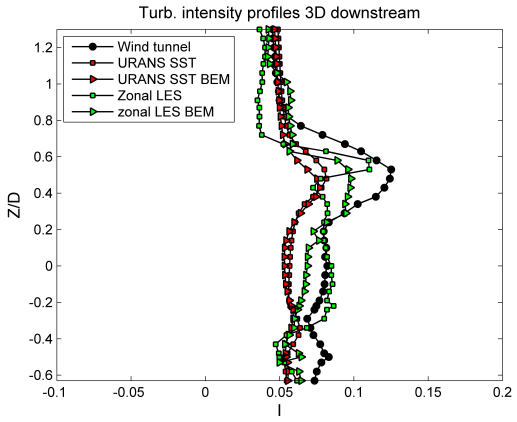

Figure 7. Normalised vertical profiles of time averaged-turbulence intensity at 3D downstream of the turbine.

Similarly, in Fig. 6 the velocity results at 3D downstream of the turbine show that the zonal LES BEM model succeeds in representing the velocity deficit at hub height, although the velocity at the tips is higher than the wind tunnel measurements. Also it can be seen that the URANS SST with BEM loses the information about local forces over the blades and produces a velocity deficit similar to the actuator disc models.

The turbulence intensity profiles in Fig. 7 also highlight that the enhancement of turbulence at the top tip is acceptably captured by the LES models, while the level of turbulence in the URANS models is lower. It can be noticed that the levels of turbulence are fairly similar for the URANS and URANS with BEM models, as it is for the LES and LES with BEM models at this location of the domain.

The results are similar at 5D downstream of the rotor, as shown in Figs. 8 and 9. While the velocity profiles present better agreement with the wind tunnel measurements in comparison to the previous locations, the models mainly under-predict the velocity deficit. In particular, as shown at 1D and 3D, the BEM models show higher velocity than those predicted using the actuator disc. In order to understand the discrepancy between the two types of models, a computation of the thrust force over the rotor has been performed using ANSYS CFX. It has been found that the overall thrust exerted by the actuator disc is $\sim$15% higher than the overall force over the non-uniformly loaded disc, explaining the different results obtained. However, the turbulence intensity levels are correctly captured by the zonal LES BEM model, while the LES actuator disc model presents some spikes that can be explained with flow instabilities and poor time-averaging of the solution.

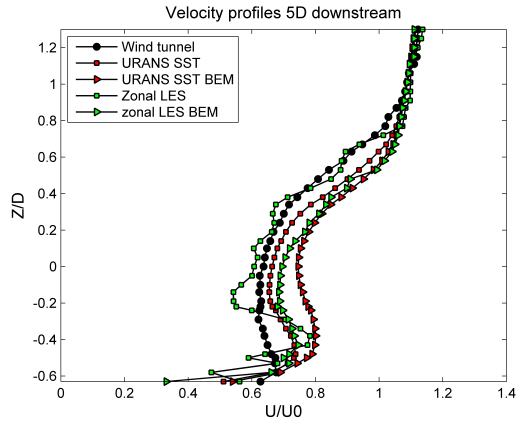

Figure 8. Normalised Vertical profiles of time averaged-velocity U/U_0 at 5D downstream of the turbine.

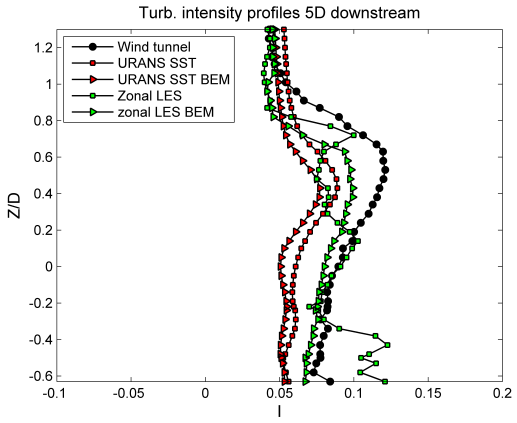

Figure 9. Normalised Vertical profiles of time averaged-turbulence intensity at 5D downstream of the turbine.

3.1. Fourier analysis

A Fourier analysis is performed to check if the LES models are acceptably resolved. The frequency spectrum for the velocity at 2D downstream of the rotor is represented in Fig. 10. The characteristic slope -5/3 [20] of all the high Reynolds turbulent jet flows is visible in the graph, confirming that the considered flow shows fully turbulent properties.

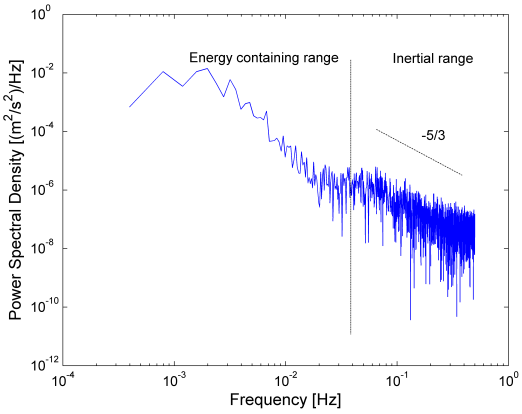

Figure 10. Power spectral density of the velocity at hub height at 2D downstream of the rotor.

4. Conclusions

In this work, Unsteady-RANS and zonal Large Eddy Simulations have been performed employing two rotor modelling techniques to distribute the force over the turbine rotor: the standard actuator disc without rotation of the flow and the actuator disc with the BEM model that accounts for rotation. Whilst the force exerted (calculated with the momentum theory) is evenly distributed over the whole rotor when using the standard actuator disc, the BEM model makes use of tabulated airfoil data at each location of the blade to compute lift and drag forces. In particular, the BEM model implements control systems through look-up tables containing turbine pitch angle and shaft angular velocity field data. The simulations have been validated with wind tunnel measurements, taking into account neutral atmospheric stability conditions. The main goal of the paper was to study and validate the generic behaviour of

the wake propagation downstream of a wind turbine in qualitative way rather than providing a detailed comparison of the wind turbine aerodynamics. Hence, it was decided to choose the wind tunnel measurements although the turbines are different Another limitation is that the flow is unidirectional in the wind tunnel experiments, while Coriolis forces are considered in the CFD simulations. The inlet wind speed direction in the CFD simulations was set-up in order to obtain an inflow direction at hub height that was consistent with the tunnel measurements. Moreover, it was found that the wake was deflected by 0.5 ° from its centreline at 5D downstream of the turbine. Hence the deflection can be considered negligible for near wake validation purposes. The results have highlighted that in the near wake the URANS models under-predict the peak of turbulence intensity at the top tip height, while the LES ones better capture the increased turbulence levels, especially when using the actuator disc incorporating BEM. It is also shown that URANS simulations reach a steady state solutions, therefore do not account for the unsteadiness of the flow. For these reasons, the LES model coupled with the rotation of the wake and an uneven distribution of the forces over the turbine better represents the wake propagation with regard to its statistical properties, although the overall force exerted by the BEM model rotor over the flow is lower than the one applied by the actuator disc. This results in the under-prediction of the velocity deficit by the BEM model in the near wake. Future work will consider the comparison of the BEM model and the actuator disc simulations so that the thrust coefficient is exactly the same. Additionally, the BEM model will be set-up without the tangential loading in order to evaluate the rotation of the wake and the non-uniform loading separately.

Acknowledgments

The authors wish to acknowledge the Engineering and Physical Sciences Research Council (EPSRC) for the financial support, E.ON New Build Technology for providing the Nysted wind farm data and Siemens Wind Power for the airfoil data. Dr Phil Hancock (University of Surrey) is gratefully acknowledged for the wind tunnel data.

References

[1] Gómez-Elvira R, Crespo A, Migoya E, Manuel F, Hernández J 2005 *J Wind Eng Ind Aerodyn* **93** pp 797–814
[2] Kasmi A E, Masson C 2008 *J Wind Eng Ind Aerodyn* **96** pp 103–122
[3] Jimenez A, Crespo A, Migoya E, Garcia J 2007 *J. Phys. Conf.* Ser **75**
[4] Jimenez A, Crespo A, Migoya E, Garcia J 2008 *Environ Res Lett* 3
[5] Calaf M, Meneveau C, Meyers J 2010 *Phys Fluids* **22**
[6] Sørensen J N, Kock C W 1995 *J. Wind Engineer. Industr. Aerodyn* **58** pp 259–275
[7] Sørensen J N, Myken A 1992 *J. Wind Engineer. Industr. Aerodyn* **39** pp 139–149
[8] Sørensen J N, Shen W Z, Munduate X 1998 *Wind Energy* **1** pp 73–78
[9] Madsen H A 1996 *10th IEA Meeting on Aerodynamics*
[10] Madsen H A, Bak C, Døssing M, Mikkelsen R, Øye S 2009 *Wind Energy* **13** pp 373–389
[11] Porté-Agel F, Lu H, Wu Y 2010 *Fifth International Symposium on Computational Wind Engineering, Chapel Hill*
[12] Hancock P E and Pascheke F 2013 *Boundary-Layer Meteorology* Springer Netherlands, DOI 10.1007/s10546-013-9887-x
[13] Menter F R 1994 *AIAA J.* **32** pp 1598–1605
[14] Menter F R, Garbaruk A and Smirnov P 2009 *Proc. 3rd Symposium on Hybrid RANS-LES Methods*
[15] Menter F R and Egorov Y 2010 ANSYS
[16] Zilitinkevich S, Johansson P E, Mironov D V, Baklanov A 1998 *J. Wind Engineer. Industr. Aerodyn* **74-76** pp 209–218
[17] WindModeller Manuals 2012 ANSYS
[18] Chamorro L, Porté-Agel F 2009 *Boundary-Layer Meteorol.* **132** pp 129–149
[19] Wu Y T, Porté-Agel F 2011 *Boundary-Layer Meteorol.* **138** DOI: 10.1007/s10546-010-9569-x
[20] Kostovinos N E 1991 *Phys. Fluids* **3(1)** pp 163–167